AIP Journal of Applied Physics

Pressure-induced ferroelectricity and enhancement of Mn-Mn exchange striction in GdMn2O5

L. H. Yin, D. H. Jang, C. B. Park, K. W. Shin, and Kee Hoon Kim

Citation: Journal of Applied Physics **119**, 104101 (2016); doi: 10.1063/1.4943587
View online: http://dx.doi.org/10.1063/1.4943587
View Table of Contents: http://scitation.aip.org/content/aip/journal/jap/119/10?ver=pdfcov
Published by the AIP Publishing

Pressure-induced ferroelectricity and enhancement of Mn-Mn exchange striction in $GdMn_2O_5$

L. H. Yin, D. H. Jang, C. B. Park, K. W. Shin, and Kee Hoon Kim[a)]
Department of Physics and Astronomy, Center for Novel States of Complex Materials (CeNSCMR) and Institute of Applied Physics, Seoul National University, Seoul 151-747, South Korea

(Received 18 January 2016; accepted 26 February 2016; published online 10 March 2016)

We report the effects of hydrostatic pressure up to $p \sim 1.73$ GPa on the multiferroic and magnetoelectric properties of $GdMn_2O_5$ single crystals. The ferroelectric (FE) polarization can be enhanced at low pressures, while it decreased after reaching a maximum at $p \sim 1.30$ GPa. This pressure induced variation of polarization can be ascribed to the combined results of Mn–Mn and Gd–Mn exchange striction under pressure. Our results show that the polarization induced by Mn–Mn interaction increases monotonously with increasing pressure and finally saturates above $p \gtrsim 1.30$ GPa. Interestingly, we find that a new FE phase appears in the temperature range of 31 K–38 K with pressure $p \gtrsim 0.88$ GPa. This new FE phase can be suppressed by magnetic field, but stabilized by pressure. The pressure-temperature (p–T) phase diagram of $GdMn_2O_5$ was obtained. Our analyses suggest that the pressure-induced new FE phase could arise from a non-collinear, incommensurate magnetic structure. © *2016 AIP Publishing LLC*.
[http://dx.doi.org/10.1063/1.4943587]

I. INTRODUCTION

Multiferroics in which ferroelectric (FE) and magnetic orders coexist have attracted much attention in recent years because of their novel physical phenomena and potential application.[1,2] The type-II multiferroics, in which ferroelectricity is induced by magnetic order, usually show large coupling among magnetism (spin), ferroelectricity (charge), and structure (lattice). In fact, giant magnetoelectric (ME) (i.e., magnetic-field-induced change of FE polarization) and/or converse ME (i.e., electric-field-induced change of magnetization) effects have been observed in numerous type-II multiferroics, such as hexaferrites $Ba_{0.52}Sr_{2.48}Co_2Fe_{24}O_{41}$,[3] $RMnO_3$ (R = rare-earth),[4] and $CoCr_2O_4$.[5] Therefore, multiferroic materials provide a playground to study a strong interaction among the three degrees of freedom, i.e., spin, charge, and lattice.

Among several mechanisms that lead to the type-II multiferroics, the symmetric spin exchange interaction, i.e., the so-called exchange-striction mechanism, has usually exhibited large spin-lattice coupling and hence relatively large spin-induced FE polarization.[6,7] Orthorhombic RMn_2O_5 (R = Bi, Y, and rare-earth) family is subject to such a mechanism, in which ferroelectricity arises from the exchange striction with a zigzag chain of Mn^{4+}–Mn^{3+}–Mn^{3+}–Mn^{4+}–Mn^{3+} along the a-axis.[8,9] A typical crystallographic and magnetic structure for RMn_2O_5 with R = Gd is shown in Fig. 1. The family of multiferroic RMn_2O_5 undergoes a common series of phase transitions as follows: a first phase transition from high-temperature (T) paramagnetic and paraelectric (PM-PE) to high-T incommensurate (HT-IC) antiferromagnetic (AFM) and paraelectric phase (termed as HT-IC-PE) appears at $T_{N1} \approx 40$–44 K, and a second transition into a commensurate (CM) AFM and FE phase (termed as CM-FE) occurs at $T_{N2} \approx 33$–39 K. Upon further temperature being lowered into $T_{N3} \approx 13$–20 K, RMn_2O_5 except R = Gd and Bi shows a transition into another low-T incommensurate AFM and FE (i.e., LT-IC-PE) state.[8–10] As expected from the origin of exchange-striction mechanism, large spin-lattice coupling has been indeed found in RMn_2O_5.[11]

It is well known that external pressure is an efficient way to control lattice and thus structure of a material.[12] It is hence expected that pressure can effectively tune magnetic and FE properties in numerous multiferroics via spin-lattice-charge coupling. Many recent studies have indeed shown that external pressure is a useful and unique tool to tune the multiferroic and ME properties.[13] For example, uniaxial pressure could control the magnetic order and ferroelectricity in a multiferroic $Ba_2CoGe_2O_7$.[14] Giant spin-driven FE polarization (up to $\sim 10\,000\ \mu C/m^2$) was also observed under high pressure in $RMnO_3$ (R = Tb, Dy, Gd).[15,16] In RMn_2O_5 (R = Y, Ho, Tb, Dy), a pressure-induced incommensurate to commensurate FE phase transition was observed at low temperatures, accompanied by large enhancement of FE polarization.[17,18]

As one of the multiferroic RMn_2O_5 compounds, $GdMn_2O_5$ exhibits unique magnetic, FE and ME behaviors as compared to other RMn_2O_5 compounds. All the rare-earth RMn_2O_5 compounds except $GdMn_2O_5$ show IC-FE phase at low temperature.[8–10] Moreover, $GdMn_2O_5$ shows the largest FE polarization ($\sim 3600\ \mu C/m^2$) and magnetic-field-tuned polarization ($\sim 5000\ \mu C/m^2$) among the RMn_2O_5 compounds. These properties are superior to most of the other multiferroics exhibiting FE polarization driven by spin order.[19] The giant tuning capability of the FE polarization is likely to be associated with the Gd–Mn exchange striction. All these

[a)]Author to whom correspondence should be addressed. Electronic mail: khkim@phya.snu.ac.kr

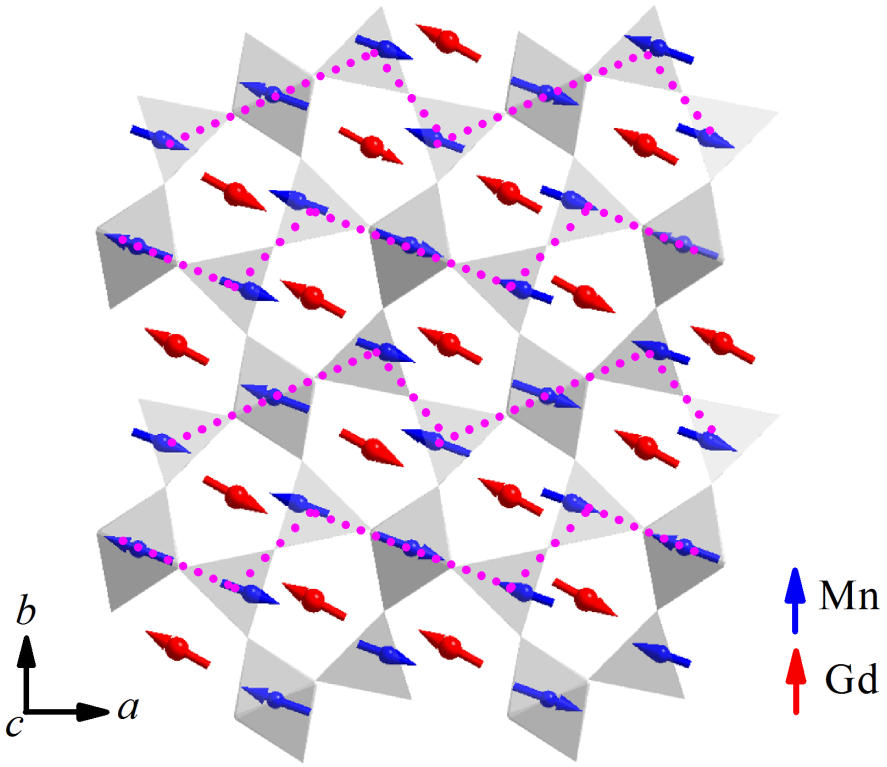

FIG. 1. A typical schematic picture of the crystallographic and magnetic structure for the RMn_2O_5 with $R = Gd$. The red and blue arrows denote the Gd and Mn spins, respectively. The red shot dashed dots show the zigzag chains of the Mn spins, the stack of which along b axis causes a polarization along b direction.

results suggest a unique role of Gd^{3+} ions with non-degenerate 4*f* orbitals ($4f^7$) on the physical properties of Gd-based oxides.

In the present work, we report the multiferroic and ME properties of $GdMn_2O_5$ crystals under hydrostatic pressure up to 1.73 GPa. Under the high pressure condition, we found greatly enhanced FE polarization and a new FE phase between T_{N2} and T_{N1} in $GdMn_2O_5$. This observation constitutes another unique multiferroic behavior of $GdMn_2O_5$ under high pressure that is distinguished from that of other RMn_2O_5.

II. EXPERIMENTAL DETAILS

$GdMn_2O_5$ single crystals were grown using the flux method as reported previously.[20] The crystals were then polished to about 0.2 mm in thickness along the *b*-axis in the orthorhombic structure, and the silver epoxy was applied on both sides of the plate-like crystals as electrical contacts. Pyroelectric/ME currents and dielectric constant were measured by using an electrometer (Keithley 617) and a capacitance bridge (AH2550A) at a frequency of 1 kHz, respectively. In the pyroelectric current measurement, the sample was first cooled down from 50 K to 2 K under a poling electric field $E_P \sim 9$ kV/cm applied along the *b*-axis and the magnetic field *H* applied along the *a*-axis. After shorting the circuit for a reasonably long duration at 2 K, the current was measured in the warming process without biased electric field. In the ME current measurements, the sample was first cooled from 50 K to a fixed temperature under $E_P \sim 9$ kV/cm, which is hereinafter referred to as the ME poling, and then ME current was collected by sweeping *H* after removing electric field. Electric polarization *P* was obtained by integrating the pyroelectric/ME currents with respect to time. Dielectric constant was also measured under warming process. Hydrostatic pressure was applied up to 1.73 GPa by a piston-type cylinder cell made of BeCu/MP35N hybrid walls. The pressure cell was loaded into the chamber of physical property measurement system (PPMS™, Quantum Design), which can provide magnetic field and controlled temperature. Daphne 7373 liquid was used as a pressure transmitting medium. Applied pressure inside the cell was estimated *in situ* by the measurements of the superconducting transition temperature of high purity lead that is located just next to the sample.[21] The magnetization measurements were carried out by using a vibrating sample magnetometer (VSM) in the PPMS™.

III. RESULTS AND DISCUSSION

Figure 2 shows the temperature dependence of FE polarization P_b along the *b*-axis under different pressures in zero magnetic field. It is observed that the onset of P_b under the ambient pressure appears around $T_{N2} \sim 34$ K, being consistent with previous reports.[19,22] With temperature lowering to $T_{N3} \sim 15$ K, P_b shows another step-like increase. Two interesting features are found in the pressure-dependent FE properties of the $GdMn_2O_5$ crystal. The first is the pressure-induced enhancement of FE polarization. As found in the lower inset of Fig. 2, P_b at 2 K, except a small decrease in the beginning, overall increases to a maximum value at $p \sim 1.3$ GPa, and then decreases again at higher pressures. This non-monotonous P_b vs *p* behavior implies different responses of the Gd–Mn and Mn–Mn interactions under pressure as will be discussed below. The second feature is that an additional small step-like increase of P_b appears at $T_X \sim 36$–38 K when $p > 0.88$ GPa, as shown in Fig. 2 and its upper inset. This immediately points to a possibility of

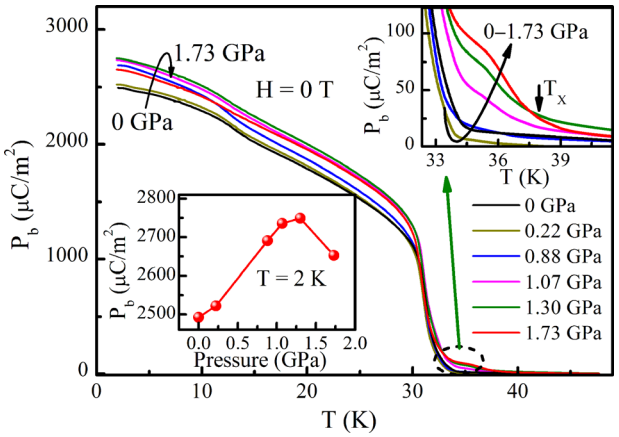

FIG. 2. Temperature-dependent FE polarization (P_b–T) along b-axis for $GdMn_2O_5$ under isotropic pressures. Lower inset shows the pressure-dependent P_b at 2 K. Upper inset shows the amplified region near $T = 36$ K.

pressure-induced new FE phase. The onset temperature T_X of this new phase as well as the polarization was further increased with pressure.

We discuss below the above two key features in $GdMn_2O_5$. Related to the first one, we need to consider the behavior of three magnetic interactions, i.e., Mn–Mn, Gd–Mn, and Gd–Gd interactions, under pressure. Figs. 3(a) and 3(b) show the pyroelectric current, FE polarization, and dielectric constant along b axis at different H in $GdMn_2O_5$. It is known that $GdMn_2O_5$ undergoes first an incommensurate, long-range AFM ordering with a propagation vector $\mathbf{k} \sim (0.49,\ 0,\ 0.18)$ due to the Mn–Mn interaction at $T_{N1} \sim 42$ K, as characterized by the abnormal increase of dielectric constant (see Fig. 3(b)).[19] Upon being cooled below $T_{N2} \sim 34$ K, Mn^{3+}/Mn^{4+} ions order in a commensurate AFM state with $\mathbf{k} = (1/2,\ 0,\ 0)$,[19] and the resulting effective magnetic field from Mn-sublattice acts on the Gd sites, leading to a weak Gd–Mn interaction. This interaction is associated with the small peak in the M–T curve (Fig. 3(c)) and the dielectric constant (Fig. 3(b)), and the onset of P_b (Fig. 3(a)). The broad peak in the M–T curve at around $T_{N3} \sim 15$ K can be ascribed to the long-range AFM ordering of Gd spins.[22] This Gd ordering temperature (~15 K) is the highest one among all the rare-earth ordering in the RMn_2O_5 family, implying a strong Gd-Gd magnetic interaction.

Figure 4 shows the isothermal magnetization vs H curves (M–H) along the a-axis at various temperatures. The large hysteresis at a high-H region (~5–7 T) in the M–H curves can be attributed to a rotation of the Gd spins since the field needed to reverse the Mn spins is much higher, e.g., above 15 T in $BiMn_2O_5$.[10] As shown in Fig. 3, a dielectric constant peak at T_{N3} is induced at a field of 8 T while the pyroelectric current peak near T_{N3} is also largely enhanced. These results can be explained as follows. The Gd spins tend to orient antiparallel to the Mn spins at zero field just below T_{N2} because of the weak Gd–Mn interaction; however, when a large enough H is applied, say, $H = 8$ T, the Gd spins rotate to the direction of H, and the polarization induced by the Gd–Mn interaction is suppressed. With temperature decreasing further at $H = 8$ T, the Gd–Mn and Gd–Gd interactions become stronger and stronger and finally overcome the

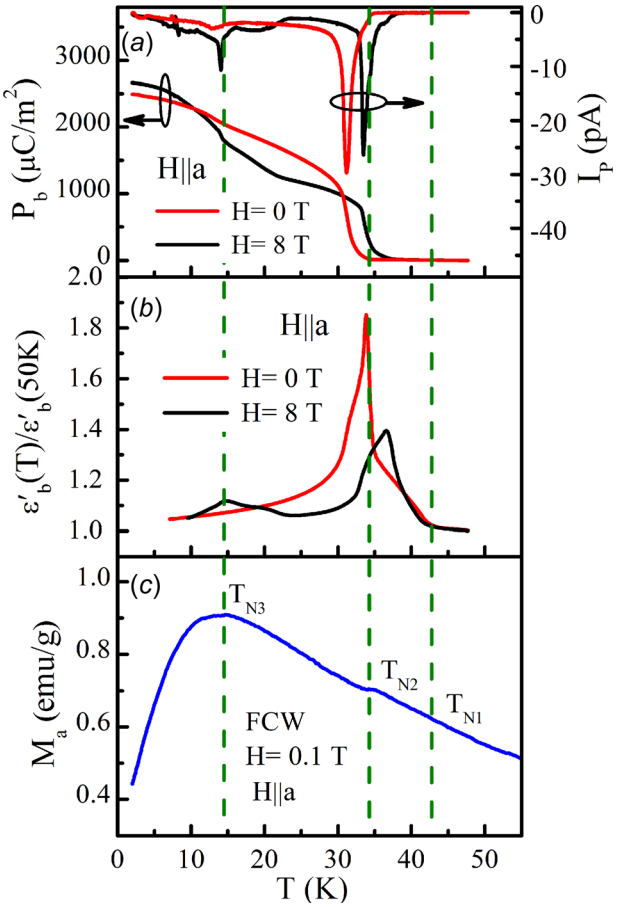

FIG. 3. (a) Temperature-dependent FE polarization P_b and pyroelectric current I_p at fields of 0 and 8 T under ambient pressure, (b) temperature-dependent relative dielectric constant ε' normalized by the value at 50 K at $H = 0$ and 8 T under ambient pressure, (c) magnetization as a function of temperature along the a-axis measured in the field-cooled warming (FCW) process under ambient pressure.

strength of the interaction between Gd/Mn and external H. Subsequently, the Gd spins reorient and order antiferromagnetically below T_{N3}, accompanied by the appearance of large additional FE polarization and a dielectric peak (see Figs. 3(a) and 3(b)).

The ferroelectricity in the RMn_2O_5 family is believed to originate from the symmetric exchange-striction mechanism

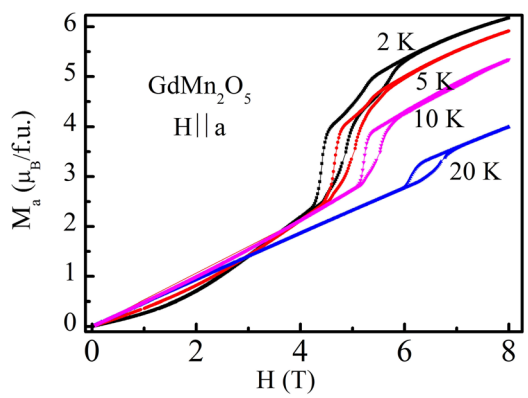

FIG. 4. Isothermal magnetic-field-dependent magnetization (M–H) along the a-axis at various temperatures under ambient pressure.

of the two *R*–Mn and Mn–Mn interactions.[8,19,23] A total FE polarization in $H = 0\,\mathrm{T}$ can be then written as $P_{\mathrm{total}} = P_{\mathrm{MnMn}} + P_{\mathrm{GdMn}}$, where P_{MnMn} is the polarization contribution from the Mn–Mn exchange striction and P_{GdMn} from the Gd–Mn exchange striction. The latter term P_{GdMn} at $T_{\mathrm{N3}} < T < T_{\mathrm{N2}}$ seems to be suppressed by a field of $H = 8\,\mathrm{T}$ as discussed above, which approximately indicates that $P_{\mathrm{GdMn}} \approx 0$ and $P_{\mathrm{total}} \approx P_{\mathrm{MnMn}}$ at $H = 8\,\mathrm{T}$.

To better understand the pressure-dependent FE polarization behavior in $GdMn_2O_5$ (Fig. 2), the P_b–T curves at $H = 8\,\mathrm{T}$ were also measured at different pressures. Figure 5 presents the FE polarization $P(H = 8\,\mathrm{T})$ (i.e., P_{MnMn}) as a function of pressure at a selected temperature of $T = 25\,\mathrm{K}$. If we assume that the P_{MnMn} term does not change too much at $0 \le H \le 8\,\mathrm{T}$, i.e., $P_{\mathrm{MnMn}}(0\,\mathrm{T}) \approx P_{\mathrm{MnMn}}(8\,\mathrm{T})$, then the $P(0\,\mathrm{T})$–$P(8\,\mathrm{T})$ can be roughly considered as P_{GdMn} term at zero field. Based on the reasoning, $(P(0\,\mathrm{T})\text{–}P(8\,\mathrm{T})) \approx P_{\mathrm{GdMn}}$ (0 T) data can be obtained as a function of pressure, as plotted in Fig. 5. It is clearly observed that P_{MnMn} shows monotonous increase with increasing pressure and begins to saturate around $p = 1.3\,\mathrm{GPa}$, while P_{GdMn} decreases overall with increasing pressure. As a combined result of such pressure-dependent variations of P_{MnMn} and P_{GdMn}, P_{total} at 25 K seems to show a rather slight increase below 0.9 GPa, a fast increase starting from ~0.9 GPa, and saturation around $p = 1.3\,\mathrm{GPa}$. The pressure-induced variation of P_b at 2 K (the lower inset of Fig. 2) seems to show qualitatively similar behavior; it slightly increases at low pressure regions, followed by a steep increase around 0.9 GPa until it shows saturation around 1.3 GPa.

It should be pointed out that the FE polarization P_{MnMn} under pressure in YMn_2O_5 of the same RMn_2O_5 family with non-magnetic Y^{3+} at *R* site does not show such monotonous enhancement like that in $GdMn_2O_5$.[18] Because of a lack of information about crystallography and magnetism under high pressure, we cannot confirm the proposed origin of the pressure-enhanced P_{MnMn} in $GdMn_2O_5$ and the different pressure-dependent behavior of P_{MnMn} in $GdMn_2O_5$ and YMn_2O_5. However, the differences in bond length and bond angle of Mn-O-Mn due to different ionic sizes of Gd^{3+} (1.053 Å) and Y^{3+} (1.019 Å) might be one possible factor to result in such different pressure effects. In the exchange striction model for ferroelectricity with up-up-down-down (↑↑↓↓) spin structure, the Hamiltonian with symmetric super-exchange interaction *J* between two magnetic moments S_i and S_j can be expressed as $H_{\mathrm{ex}} = J(r_{ij}, \theta)S_i \cdot S_j$, where r_{ij} and θ denote the bond length and bond angle, respectively. The FE polarization can be effectively affected by applied pressure via changing the r_{ij} and θ between S_i and S_j. Therefore, in the case of $GdMn_2O_5$, the shortened r_{ij} and varied θ of Mn-O-Mn induced by pressure may contribute to the monotonous enhancement of P_{MnMn}.

We now discuss the second interesting feature under pressure, i.e., pressure induced new phase. In order to get more information on the new phase, the temperature-dependent dielectric constant ε' under different pressures was measured and presented in Fig. 6(a). With an increase in the pressure, the peak shown in the dielectric constant near T_{N2} is gradually suppressed and shifts toward lower temperatures. When the applied pressure is higher than ~0.88 GPa, another dielectric peak appears above T_{N2}, becomes stronger, and shifts to higher temperature with the increase in the pressure. The temperature T_{X} of the new dielectric constant peak is the same as the onset of FE polarization due to the new phase, as can be clearly observed in the selected $p = 1.73\,\mathrm{GPa}$ in Fig. 6(b) and its inset. The simultaneous occurrence of the FE polarization and dielectric

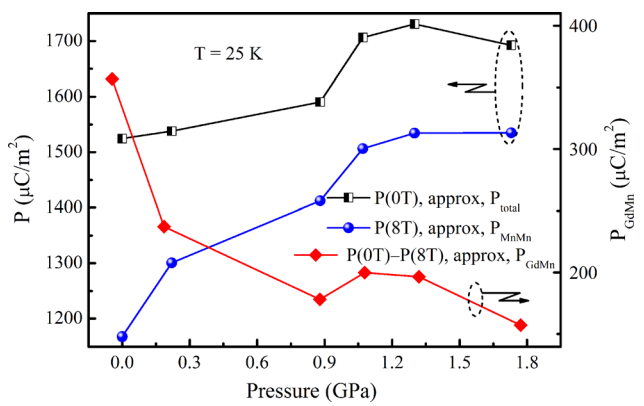

FIG. 5. Pressure-dependence of FE polarizations at $T = 25\,\mathrm{K}$, $P(8\,\mathrm{T})$, $P(0\,\mathrm{T})$-$P(8\,\mathrm{T})$, and $P(0\,\mathrm{T})$, which can approximately represent the polarization contributions due to Mn-Mn interaction (P_{MnMn}), Gd–Mn interactions (P_{GdMn}), and their total sum (P_{Total}).

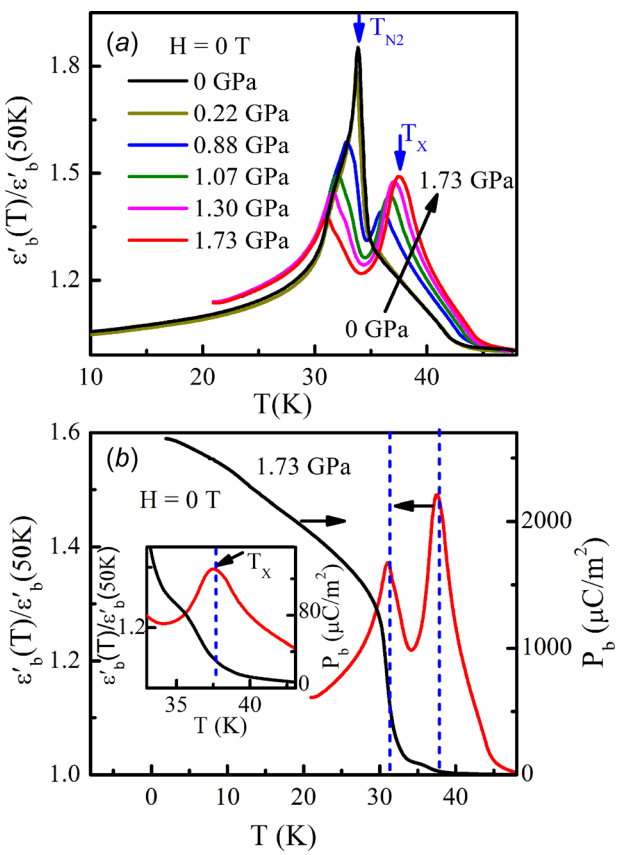

FIG. 6. (a) Normalized relative dielectric constant as a function of temperature (i.e., $\varepsilon'(T)/\varepsilon'(50\,\mathrm{K})$–$T$) at $H = 0\,\mathrm{T}$ under different pressures; (b) $\varepsilon'(T)/\varepsilon'(50\,\mathrm{K})$–$T$ and P_b–T under pressure $p = 1.73\,\mathrm{GPa}$. The inset is the locally magnified image.

peak demonstrates that the new phase induced by pressure is indeed ferroelectric.

To elucidate the magnetic-field effect on the FE polarization and dielectric constant ε' in this new FE phase, the ME effect (P–H) and the magnetodielectric (MD) effect (i.e., $(\Delta\varepsilon'(H)/\varepsilon'(0)$–$H)$) were investigated both in the new FE phase (termed as the FE2 phase) and in the CM-FE phase after the ME poling, as shown in Fig. 7. In the CM-FE, a sharp anomaly in the dielectric constant and a drop in the FE polarization were observed in the vicinity of ~5 T at $T = 25$ K under ambient pressure. As discussed above, the P–H and $\Delta\varepsilon'(H)/\varepsilon'(0)$–$H$ behavior in the CM-FE phase at 25 K can be ascribed to the H-induced Gd-spin reorientation and suppression of the P_{GdMn}. On the other hand, in the FE2 phase, an anomaly in $\Delta\varepsilon'(H)/\varepsilon'(0)$–$H$ and a minimum in P–H occurred near ~5 T at $T = 35$ K under $p = 1.73$ GPa. In the FE2 phase, the polarization first decreases with increasing H and reaches a minimum at ~5 T, then increases again above ~5 T. This indicates that the ferroelectricity in the FE2 phase can be suppressed by H and that it transforms into the phase with higher electric polarization for $H \gtrsim 5$ T. This implies that the FE2 phase might be noncollinear, incommensurate spin structure at a low field region and becomes a gradually collinear, commensurate phase at a high field region above 5 T. It is well known that a magnetic field usually suppresses the non-collinear spin configuration, and in fact, in $R\mathrm{Mn_2O_5}$ (R = Y, Ho, Dy, Tb), the magnetic field can induce a transition from the low-temperature, incommensurate magnetic order into the commensurate one.[24] The H-induced transition from a non-collinear incommensurate AFM spin structure into a collinear AFM state was also observed in the well-known $BiFeO_3$.[25,26]

Based on the above results, we propose that the ferroelectricity in the FE2 phase in $GdMn_2O_5$ could be of spin-current origin with a non-collinear, incommensurate magnetic structure, instead of exchange-striction origin, coming from the collinear magnetic structure as that in the CM-FE phase. We notice that most of the compounds in the $R\mathrm{Mn_2O_5}$ (R = Y, Tb, etc.) family show a re-entrance of incommensurate FE (LT-IC-FE) phase at temperatures below CM-FE phase with contracted lattice, implying that the energy of LT-IC-FE spin state is somewhat lower than the CM-FE phase. The lattice compression by applied pressure in $GdMn_2O_5$ may have similar effect on the magnetic structure transition as compared to the low-temperature induced lattice contraction in $R\mathrm{Mn_2O_5}$ (R = Y, Tb, etc.) compounds. In this sense, a new incommensurate spin state out of CM-FE by applying pressure is possibly energetically favorable in $GdMn_2O_5$. Therefore, the incommensurate structure in the FE2 phase in $GdMn_2O_5$ is likely similar to the LT-IC-FE state in other $R\mathrm{Mn_2O_5}$ (R = Y, Tb, etc.) compounds, where the magnetization of the Mn ions in each zigzag chain is modulated along the a axis and spins in every other chain are rotated slightly toward the b axis.[8,27] It is also important to note that both the FE polarization and the FE transition temperature T_X in the FE2 phase can be enhanced by the external pressure, as can be seen in the upper inset of Fig. 2. The transition temperature T_{N1} of the IC-PE phase was also enhanced with the increasing pressure (see Figs. 6(a) and 8). This pressure-induced stabilization of both FE2 and IC-PE phases implies that these two phases may have similar incommensurate magnetic structure, providing further evidence for the possible non-collinear incommensurate magnetic structure in the new FE phase below T_X. The

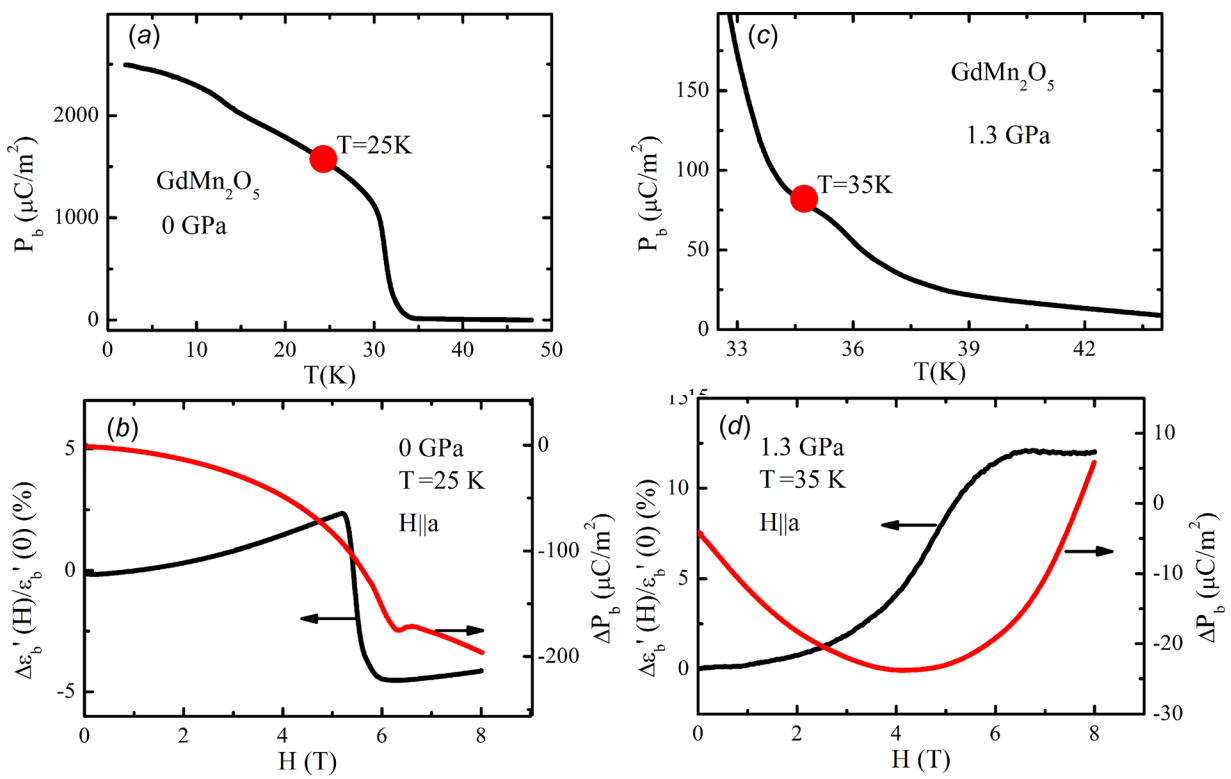

FIG. 7. (a) and (c) P_b–T under ambient and 1.30 GPa, respectively; (b) and (d) ME and MD effects at 25 K under ambient pressure and at 35 K under 1.30 GPa, respectively.

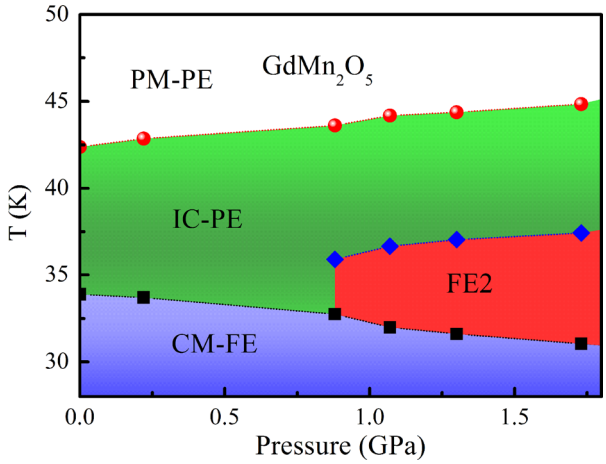

FIG. 8. Pressure–temperature (p–T) phase diagram based on the dielectric data of the $GdMn_2O_5$ single crystal.

test for our proposed scenario needs to await further structural investigations under high pressure.

The pressure-temperature (p–T) phase diagram derived from the dielectric data for $GdMn_2O_5$ is shown in Fig. 8. One of the common multiferroic features for the RMn_2O_5 (R = Y, Bi, and rare-earth) families is to show the same phase-sequence of PM-PE, HT-IC-PE (below T_{N1}), and CM-FE (below T_{N2}) upon cooling. However, the p–T phase diagram of $GdMn_2O_5$ shown in Fig. 8 is very different from those of other RMn_2O_5 (R = Y, Ho, etc.) compounds.[17,18] In RMn_2O_5 (R = Y, Ho, Tb, Dy), the pressure only induces a transition of LT-IC-FE into CM-FE phase at low temperatures and no new phase above T_{N2}, while in $GdMn_2O_5$ pressure induces a new FE2 phase between CM-FE and IC-PE phases. This difference in the p–T phase diagram may arise from two possible aspects: (1) the ionic size of Gd^{3+} is larger than those of Y^{3+} and Tb^{3+}–Tm^{3+}, resulting in different R–Mn and Mn–Mn interactions. In fact, the commensurate phase CM-FE in RMn_2O_5 with rare-earth elements with relatively small ionic radius (R = Y, Tb–Tm) can be characterized by a vector $\mathbf{k} = \{1/2, 0, 1/4\}$, whereas the CM-FE phase with larger ionic radius R may show slightly different vector $\mathbf{k}$.[28] For instance, R = Bi shows a $k_z = 1/2$ and R = Gd shows a $k_z = 0$.[19] (2) The Gd^{3+} ions with non-degenerate orbitals with seven 4f valence-electrons may also play a unique role in the spin-lattice coupling and f–d spin interaction between Gd and Mn in $GdMn_2O_5$, which still awaits further investigation. It is noteworthy that the unique role of Gd^{3+} ions, as compared to other rare-earth ions, has also been observed in many other magnetic materials.[29,30]

IV. CONCLUSIONS

The multiferroic and ME properties under isotropic pressure up to $p \sim 1.73$ GPa were studied in the $GdMn_2O_5$ single crystal. The ferroelectricity was enhanced under low and intermediate pressures. The FE polarization reached a maximum at $p \sim 1.30$ GPa and then decreased at higher pressures, which can be attributed to the combined effect of different pressure-dependent polarizations induced by exchange striction from the Gd–Mn and Mn–Mn interactions. When the external pressure is higher than ~0.88 GPa, a new FE phase between IC-PE and CM-FE phases in the temperature range of 31 K–38 K was found. The magnetic-field-induced suppression and pressure-induced stabilization indicate a non-collinear incommensurate magnetic structure in this new FE phase. Our results show that the external pressure is a useful and effective tool to explore new multiferroic phases.

Note added in proof. Upon completion of the research and writings, we become aware of a recent publication on the pressure studies of $GdMn_2O_5$, which reveals p–T phase diagram similar to ours but with a different proposal for the origin of the pressure induced FE2 phase.[31]

ACKNOWLEDGMENTS

This study was supported by Creative Research Initiative (2010-0018300) by Korean Government.

[1]R. Ramesh and N. A. Spaldin, Nat. Mater. **6**, 21 (2007).
[2]H. Schmid, J. Phys.: Condens. Matter **20**, 434201 (2008).
[3]S. H. Chun *et al.*, Phys. Rev. Lett. **108**, 177201 (2012).
[4]T. Kimura, T. Goto, H. Shintani, K. Ishizaka, T. Arima, and Y. Tokura, Nature **426**, 55 (2003).
[5]Y. Yamasaki, S. Miyasaka, Y. Kaneko, J.-P. He, T. Arima, and Y. Tokura, Phys. Rev. Lett. **96**, 207204 (2006).
[6]V. Caignaert *et al.*, Phys. Rev. B **88**, 174403 (2013).
[7]Y. Tokunaga, S. Iguchi, T. Arima, and Y. Tokura, Phys. Rev. Lett. **101**, 097205 (2008).
[8]A. B. Sushkov, M. Mostovoy, R. V. Aguilar, S. W. Cheong, and H. D. Drew, J. Phys.: Condens. Matter **20**, 434210 (2008).
[9]N. Hur, S. Park, P. A. Sharma, J. S. Ahn, S. Guha, and S. W. Cheong, Nature **429**, 392 (2004).
[10]J. W. Kim *et al.*, Proc. Natl. Acad. Sci. U. S. A. **106**, 15573 (2009).
[11]C. R. dela Cruz, F. Yen, B. Lorenz, M. M. Gospodinov, C. W. Chu, W. Ratcliff, J. W. Lynn, S. Park, and S. W. Cheong, Phys. Rev. B **73**, 100406 (2006).
[12]J. Ruiz-Fuertes, A. Friedrich, O. Gomis, D. Errandonea, W. Morgenroth, J. A. Sans, and D. Santamaria-Perez, Phys. Rev. B **91**, 104109 (2015).
[13]C. dela Cruz, F. Yen, B. Lorenz, Y. Q. Wang, Y. Y. Sun, M. M. Gospodinov, and C. W. Chu, Phys. Rev. B **71**, 060407 (2005).
[14]T. Nakajima, Y. Tokunaga, V. Kocsis, Y. Taguchi, Y. Tokura, and T.-H. Arima, Phys. Rev. Lett. **114**, 067201 (2015).
[15]T. Aoyama, K. Yamauchi, A. Iyama, S. Picozzi, K. Shimizu, and T. Kimura, Nat. Commun. **5**, 4927 (2014).
[16]T. Aoyama, A. Iyama, K. Shimizu, and T. Kimura, Phys. Rev. B **91**, 081107 (2015).
[17]C. R. dela Cruz, B. Lorenz, Y. Y. Sun, Y. Wang, S. Park, S. W. Cheong, M. M. Gospodinov, and C. W. Chu, Phys. Rev. B **76**, 174106 (2007).
[18]R. P. Chaudhury, C. R. dela Cruz, B. Lorenz, Y. Sun, C.-W. Chu, S. Park, and S.-W. Cheong, Phys. Rev. B **77**, 220104 (2008).
[19]N. Lee, C. Vecchini, Y. J. Choi, L. C. Chapon, A. Bombardi, P. G. Radaelli, and S. W. Cheong, Phys. Rev. Lett. **110**, 137203 (2013).
[20]B. M. Wanklyn, J. Mater. Sci. **7**, 813 (1972).
[21]T. Smith and C. Chu, Phys. Rev. **159**, 353 (1967).
[22]S. I. Vorob'ev, A. L. Getalov, E. I. Golovenchits, E. N. Komarov, V. P. Koptev, S. A. Kotov, I. I. Pavlova, V. A. Sanina, and G. V. Shcherbakov, Phys. Solid State **55**, 466 (2013).
[23]Z. Y. Zhao, M. F. Liu, X. Li, L. Lin, Z. B. Yan, S. Dong, and J. M. Liu, Sci. Rep. **4**, 3984 (2014).
[24]H. Kimura, Y. Kamada, Y. Noda, K. Kaneko, N. Metoki, and K. Kohn, J. Phys. Soc. Jpn. **75**, 113701 (2006).
[25]B. Ruette, S. Zvyagin, A. P. Pyatakov, A. Bush, J. F. Li, V. I. Belotelov, A. K. Zvezdin, and D. Viehland, Phys. Rev. B **69**, 064114 (2004).
[26]L. H. Yin, J. Yang, B. C. Zhao, Y. Liu, S. G. Tan, X. W. Tang, J. M. Dai, W. H. Song, and Y. P. Sun, J. Appl. Phys. **113**, 214104 (2013).
[27]G. Blake, L. Chapon, P. Radaelli, S. Park, N. Hur, S. Cheong, and J. Rodriguez-Carvajal, Phys. Rev. B **71**, 214402 (2005).

[28]Y. Noda, H. Kimura, M. Fukunaga, S. Kobayashi, I. Kagomiya, and K. Kohn, J. Phys.: Condens. Matter **20**, 434206 (2008).
[29]Y. Tokunaga, N. Furukawa, H. Sakai, Y. Taguchi, T. H. Arima, and Y. Tokura, Nat. Mater. **8**, 558 (2009).
[30]L. H. Yin, J. Yang, X. C. Kan, W. H. Song, J. M. Dai, and Y. P. Sun, J. Appl. Phys. **117**, 133901 (2015).
[31]N. Poudel, M. Gooch, B. Lorenz, C. Chu, J. Kim, and S. Cheong, Phys. Rev. B **92**, 144430 (2015).